JOURNAL OF Applied Polymer SCIENCE

A Superabsorbent Nanocomposite Based on Sodium Alginate and Illite/Smectite Mixed-Layer Clay

Yizhe Wang,[1,2] Wenbo Wang,[1,3] Xiaoning Shi,[1,2] Aiqin Wang[1,3]

[1]Center of Eco-material and Green Chemistry, Lanzhou Institute of Chemical Physics, Chinese Academy of Sciences, Lanzhou, People's Republic of China

[2]Graduate University of the Chinese Academy of Sciences, Beijing, People's Republic of China

[3]R&D Center of Xuyi Attapulgite Applied Technology, Lanzhou Institute of Chemical Physics, Chinese Academy of Science, Lanzhou, People's Republic of China

Correspondence to: A. Wang (E-mail: aqwang@licp.cas.cn)

ABSTRACT: A series of superabsorbent nanocomposites were prepared by free radical grafting copolymerization of sodium alginate, partially neutralized acrylic acid (AA), styrene, and illite/smectite mixed-layer clay (I/S). The structure and morphology of the nanocomposites were confirmed by Fourier transform infrared spectroscopy, X-ray diffraction, and scanning electron microscope techniques. It was shown that the incorporation of I/S clearly enhanced the swelling properties of the nanocomposites. Various salts and surfactants showed remarkable effects on the swelling behaviors of the nanocomposites. Moreover, the nanocomposite exhibited better responsive and reversible on–off switching characteristics in pH 7.0 and 2.0 buffer solutions, which renders it promising for drug delivery application. © 2013 Wiley Periodicals, Inc. J. Appl. Polym. Sci. 000: 000–000, 2013

KEYWORDS: composites; gels; swelling

Received 20 November 2012; accepted 7 February 2013; published online
DOI: 10.1002/app.39141

INTRODUCTION

Superabsorbents are moderately crosslinked three-dimensional network hydrophilic polymer materials with the capability to absorb and retain large quantities of aqueous solutions compared with general absorbing materials. Owing to the excellent water-swellable characteristic, superabsorbents were extensively applied in agriculture and horticulture,[1,2] hygiene products,[3] wastewater treatment,[4] catalyst supports,[5] and drug delivery.[6] However, the conventional petroleum-based synthetic superabsorbents were limited in some application fields due to their high cost, latent toxic effect, and serious environmental impact. Therefore, the design and developments of the superabsorbents based on naturally available raw materials have attracted considerable interests. Among them, the natural polysaccharides with renewable, nontoxic, and biodegradable advantages (i.e., starch,[7] chitosan,[8] cellulose,[9] tara gum,[10] konjac glucomannan,[11] and guar gum[12]) and the inorganic clay minerals with low cost and abundance superiorities (i.e., bentonite,[13] attapulgite,[14] rectorite,[12] vermiculite,[15] and kaolin[16]) were especially concerned. Furthermore, the organic–inorganic nanocomposites derived from polysaccharides and clays have been honored as the promising materials in "greening the 21st century materials world" by virtue of their excellent properties and good commercial and environmental values.[17]

Alginate derived from brown algae is an anionic natural linear polymer composed of α-1,4-L-glucuronic acid (G units) and poly-β-1,4-D-mannuronic acid (*M* units) in varying proportions by one to four linkages. Its carboxyl and hydroxyl groups on the backbone may provide hydrophilicity for superabsorbents. In addition, alginate can be facilely modified through grafting copolymerization with various hydrophilic vinyl monomers to derive superabsorbent materials with higher swelling capacity.[18,19]

Illite/smectite mixed-layer clay (I/S) is traditionally thought of as a mixture of crystallites that contain illite and smectite as two distinct, interstratified mineral entitles.[20] I/S is produced from the illitization of smectite which is one of the most frequent mineral reactions occurring in deeply buried sedimentary environments, and so it has the dual characteristics of illite and smectite.[21] There are reactive –OH groups on the surface of I/S, and these groups are accessible to prepare organic–inorganic superabsorbent composites. However, rare research regards to the compounding of I/S into superabsorbent hydrogels.

For improving the properties of the alginate-based superabsorbent and studying the effect of the I/S clay on the structure and swelling properties of the superabsorbent, the new superabsorbent nanocomposite sodium alginate-*g*-poly(sodium acrylate-*co*-styrene)/illite/smectite mixed-layer clays (NaAlg-*g*-p(AA-*co*-St)/I/S) was prepared. The network structures of the developed nanocomposites were characterized by Fourier transform infrared spectroscopy (FTIR), X-ray diffraction (XRD), and scanning electron microscope (SEM) techniques. The content of I/S were optimized to obtain the maximum swelling capacity. Finally, the effects of various salts, surfactants, and pH medium on the swelling behaviors were studied systematically.

EXPERIMENTAL

Materials

Sodium alginate (NaAlg) was purchased from Shanghai Chemical Reagents Corp. (Shanghai, China). I/S, with the composition of 18.27% Al_2O_3, 1.870% MgO, 0.227% CaO, 65.93% SiO_2, 3.147% K_2O, and 3.526% Fe_2O_3, was obtained from Shangsi, Guangxi, China. Acrylic acid (AA, Chemically pure, Shanghai Shanpu Chemical Factory, Shanghai, China) was distilled under reduced pressure before use. Sodium *n*-dodecyl sulfate (SDS) was supplied by the Shanghai Chemical Reagent Corp. (Shanghai, China). Styrene (St, Chemically pure, Shantou Xilong Chemical Factory, Shantou, China), ammonium persulfate (APS, Analytical grade, Tianjin Chemical Reagent Co., Tianjin, China), and *N*,*N*′-methylenebisacrylamide (MBA, Chemically pure, Shanghai Yuanfan Auxiliaries Co., Shanghai, China) were used as received. Cetyltrimethylammonium bromide (CTAB, Beijing Chemical Reagents Company, China) and dodecyltrimethylammonium bromide (DTAB, Beijing Chemical Reagents Company, China) were used as purchased. The other reagents used were all analytical grade, and all solutions were prepared with deionized water.

Preparation of the Superabsorbent Nanocomposite

NaAlg (1.20 g) was dissolved in 20 mL distilled water in a 250 mL four-necked flask equipped with a mechanical stirrer, a reflux condenser, a nitrogen line, and a thermometer. The flask was heated to 60°C and kept for 0.5 h under continuous N_2 purging to remove the dissolved oxygen. Then, 10 mL of the aqueous solution containing 2.4 mg surfactant (SDS) was added, and the system was remained at 60°C for 0.5 h. After that, 5 mL of the aqueous solution of APS (0.10 g) was added to the mixture and stirred for 15 min. Subsequently, the reaction system was cooled to 40°C, and the mixture solution containing AA (7.20 g, partially neutralized by 8.8 mL 8 *M* NaOH solution), St (0.15 g), MBA (0.0216 g), and proper amount of I/S was added. The oil bath was slowly heated to 70°C and kept for 3 h to complete the reaction. The resulted gel products were firstly frozen in icebox (−22°C) for 10 h. Then, the freezing gels were washed thoroughly with ethanol/water mixture (7 : 3, v/v) for several times to remove the surfactant and finally soaked into absolute ethanol for 24 h to dewatering. The products were filtrated out and dried at room temperature. The dry samples were used after ground and passed through 40–80 mesh sieve (180–380 μm).

Measurement of Swelling Capacity

The accurately weighed 0.05 g of xerogel was immersed in 250 mL of distilled water or 0.9 wt % NaCl aqueous solution and swelled at room temperature for 3 h. The swollen hydrogel was separated from the nonabsorbed water by filtrating through a 100-mesh sieve and then weighed. The water absorption was calculated by the following equation:

$$Q_{eq} = (m - m_1)/m_1 \quad (1)$$

where m (g) is the mass of the swollen hydrogel, and m_1 (g) is the mass of the xerogel. The swelling capacity of the sample in saline solution and surfactant solution was tested by the same procedure.

Measurement of Swelling Kinetics

0.05 g xerogel was placed into a beaker containing 250 mL distilled water. The swollen hydrogel was filtrated and weighed in set intervals, and the water absorption at corresponding time was calculated by using eq. (1).

The time-dependent swelling behaviors of the sample in saline solution were measured by the method similar to that in distilled water.

Evaluation of pH-Sensitivity

The solutions with pH 2.0 and 7.0 were prepared by diluting HCl (pH 1.0) and NaOH (pH 13.0) solutions. The pH value of the solutions was determined by a pH meter (DELTA-320). The pH-sensitivity of the superabsorbent nanocomposite was investigated in terms of its swelling and deswelling in two buffer solutions with pH 7.0 and 2.0, respectively. The consecutive time interval for each swelling–deswelling cycle is 40 min.

Characterization

FTIR spectra were determined by a Nicolet NEXUS FTIR spectrometer in 4000–400 cm^{-1} wavenumber region using KBr pellets. XRD analyses were performed using an X-ray power diffractometer with Cu anode (PANalytical Co. X'pert PRO), running at 40 kV and 30 mA, scanning from 4° to 13°. The morphologies of the samples were investigated using a JSM-6701F field emission SEM (JEOL) after coating the sample with gold film.

RESULTS AND DISCUSSION

FTIR Analysis

The FTIR spectra of (a) NaAlg, (b) NaAlg-*g*-p(AA-*co*-St), (c) I/S, and (d) NaAlg-*g*-p(AA-*co*-St)/I/S are illustrated in Figure 1. As can be seen, NaAlg showed the characteristic absorption band of C–OH groups at 1032 cm^{-1} [Figure 1(a)]. After reaction, this band was weakened and the new absorption bands at 1746 cm^{-1} (C=O stretching vibration of –COOH groups), 1628 cm^{-1} (asymmetrical stretching vibration of $–COO^-$ groups), 1465 cm^{-1}, and 1408 cm^{-1} (symmetrical stretching vibration of $–COO^-$ groups) were appeared in the spectrum of NaAlg-*g*-p(AA-*co*-St) [Figure 1(b)]. This indicated that AA monomers had grafted onto the NaAlg backbones. As shown in Figure 1(d), the characteristic absorption band of –OH groups on the surface of I/S clays at 3699 and 3623 cm^{-1} was disappeared [Figure 1(c)], which revealed that the I/S took

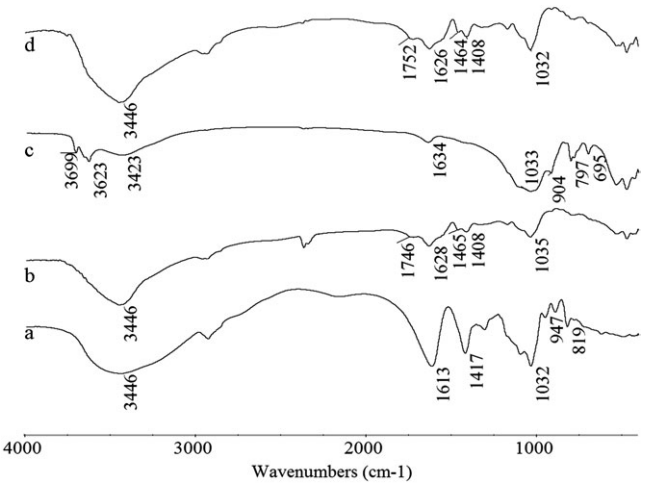

Figure 1. FTIR spectra of (a) NaAlg, (b) NaAlg-*g*-p(AA-*co*-St), (c) I/S, and (d) NaAlg-*g*-p(AA-*co*-St)/I/S.

participated in the graft polymerization. The characteristic absorption band of St cannot be observed in FTIR spectra [Figure 1(b,d)] owing to the tiny content of St in hydrogels. The existence of St in the hydrogel has been proved by UV–vis analysis.[22] All these information confirmed the grafting copolymerization reaction and the formation of nanocomposite structure.

XRD Analysis

XRD profiles of I/S and NaAlg-*g*-p(AA-*co*-St)/I/S (2.5 and 10 wt %) are presented in Figure 2. The XRD pattern of I/S [Figure 2(a)] shows the reflections at $2\theta = 5.88°$ ($d = 1.453$ nm), 8.74° ($d = 0.987$ nm), and 12.27° ($d = 0.71$ nm), which can be attributed to the characteristic diffraction of smectite, illite, and kaolin mineral, respectively. However, the diffraction peaks disappeared after forming nanocomposite [Figure 2(b, c)]. As is well known, the change in interlayer spacing (d) from XRD analysis is the criterion to identify the intercalated or exfoliated structure of layered silicates in a nanocomposite.[23] Thus, these changes of XRD curves demonstrated that I/S clay was exfoliated and dispersed in the superabsorbent nanocomposite with a nanoscale platelet. The similar result can also be observed in the nanocomposite superabsorbent starch grafted poly(acrylic acid-*co*-acrylamide)/montmorillonite [P(AA-*co*-AM)/MMT].[24]

SEM Analysis

The addition of I/S clay to the NaAlg-*g*-p(AA-*co*-St) hydrogel could change its structure and morphology as depicted in Figure 3. It was clearly observed that I/S clay presented obvious bedded structure [Figure 3(a)], and NaAlg-*g*-p(AA-*co*-St) hydrogel only exhibited a flat and dense surface [Figure 3(b)]. However, the nanocomposites containing I/S clay showed a correspondingly crumpled and coarse surface [Figure 3(c,d)], and the surface roughness of NaAlg-*g*-p(AA-*co*-St)/I/S (2.5 wt %) was higher than NaAlg-*g*-p(AA-*co*-St)/I/S (10 wt %). This suggested that the incorporation of proper amount of I/S was benefit to improve the surface structure of the nanocomposite. Furthermore, the images also gave a direct observation that I/S was uniformly dispersed in the polymer matrix with a good interface compatibility. This is in agreement with the XRD results that I/S was exfoliated as nanoscale platelets during the polymerization process.

Effect of I/S Content on Swelling Capacity

I/S content not only influenced the composition and structure of the superabsorbent nanocomposite but also affected its swelling properties. As shown in Figure 4, the swelling capacity of the nanocomposite was enhanced to 810 g g^{-1} with increasing the I/S content to 2.5 wt %. The desirable improvement of swelling capacity can be attributed the fact that I/S participated in polymerization reaction through the active –OH groups on its surface. As shown in SEM observation, the incorporation of I/S improved the surface structure and contact area, which is convenient for the penetration of water into the polymer network. In addition, the rigid I/S platelets can prevent intertwining of polymer chains and reduce the hydrogen-bonding interaction among hydrophilic groups. This decreased the degree of physical crosslinking and thus contributed to improve the swelling capacity. However, the swelling capacity gradually decreased with the further increase of I/S content above 2.5 wt %. This may be due to that excess I/S increased the viscosity of polymerization system and decreased the molecular collision, for which the polymerization process was interfered and the three-dimensional network cannot be formed efficiently. As a result, the swelling capacity was decreased. Furthermore, excess I/S was physically filled in the polymer matrix and obstructed the network space. This decreased the hydrophilicity of the composite and is adverse to holding water of network voids. The similar tendency can be observed for other superabsorbent composites.[25]

Swelling Kinetics

Figure 5 shows the swelling curves of superabsorbents as a function of time. At initial stage (<900 s), the swelling ratio increased rapidly, and then the increase degree was slowed down. For analyzing the effect of I/S content on the swelling kinetics, Schott's second-order swelling kinetic model was introduced [eq. (2)][26,27]:

$$t/Q_t = A + Bt \quad (2)$$

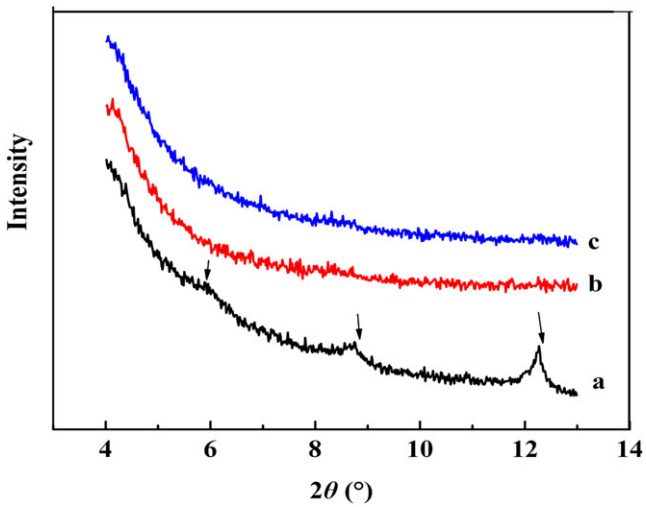

Figure 2. XRD profiles of (a) I/S, (b) NaAlg-*g*-p(AA-*co*-St)/I/S (2.5 wt %), and (c) NaAlg-*g*-p(AA-*co*-St)/I/S (10 wt %). [Color figure can be viewed in the online issue, which is available at wileyonlinelibrary.com.]

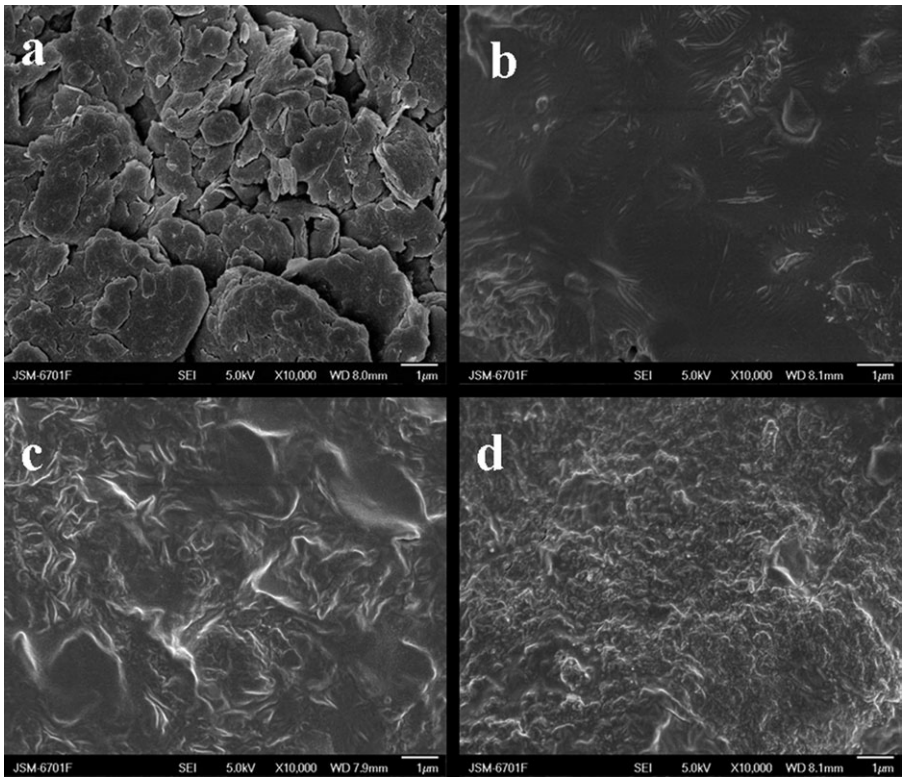

Figure 3. SEM images of (a) I/S, (b) NaAlg-*g*-p(AA-*co*-St), (c) NaAlg-*g*-p(AA-*co*-St)/I/S (2.5 wt %), and (d) NaAlg-*g*-p(AA-*co*-St)/I/S (10 wt %).

where A and B are the two coefficients whose physical sense is interpreted as follows. At a long contact time $Bt \gg A$, that is, it is the reciprocal of the maximum or equilibrium swelling capacity. On the contrary, at a very short contact time $A \gg Bt$, and in the limit, eq. (2) becomes

$$\lim_{t \to 0}(dQ_t/dt) = 1/A \tag{3}$$

Therefore, the intercept A is the reciprocal of the initial swelling rate. Thus, eq. (2) can be expressed as follows:

$$t/Q_t = 1/K_{is} + (1/Q_\infty)t \tag{4}$$

Here, Q_t (g g^{-1}) is the swelling ratio at a given time t (s), Q_∞ (g g^{-1}) is the theoretical equilibrium swelling ratio, and K_{is} (g g^{-1} s^{-1}) is the initial swelling rate constant. On the basis of the experimental data, we can get a set of straight lines (t/Q_t against time t, Figure 6) with good linear correlation coefficient. This indicates that Schott's theoretical swelling model is suitable for evaluating the swelling kinetics of the superabsorbents. The calculated swelling kinetic parameters are listed in Table I. It can be seen that the swelling rate of the superabsorbents was in the order: NaAlg-*g*-p(AA-*co*-St)/I/S (2.5 wt %) > NaAlg-*g*-p(AA-*co*-St)/I/S (5 wt %) > NaAlg-*g*-p(AA-*co*-St) > NaAlg-*g*-p(AA-*co*-St)/

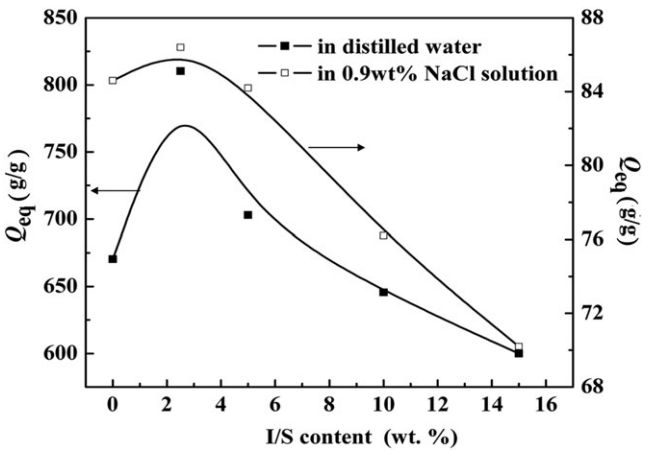

Figure 4. Effect of I/S content on swelling capacity.

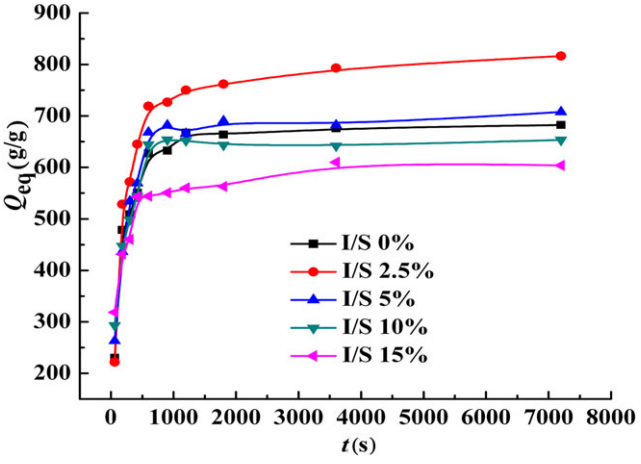

Figure 5. Effect of I/S content on swelling rate. [Color figure can be viewed in the online issue, which is available at wileyonlinelibrary.com.]

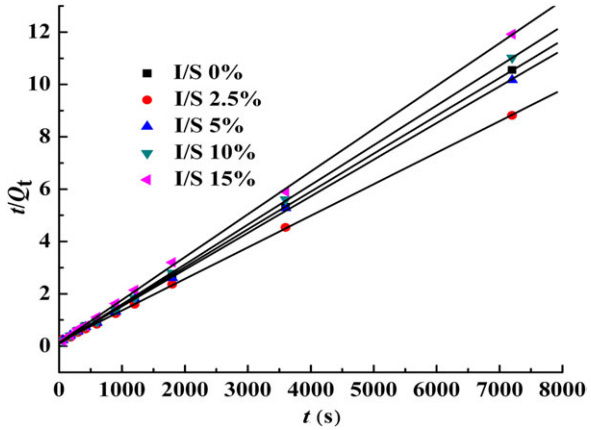

Figure 6. Swelling kinetic fitting curves of the nanocomposites with different contents of I/S. [Color figure can be viewed in the online issue, which is available at wileyonlinelibrary.com.]

I/S (10 wt %) > NaAlg-*g*-p(AA-*co*-St)/I/S (15 wt %). This revealed that the addition of moderate amount of I/S contributes to improve the surface and interior structure of the sample, which is benefit for increasing the diffusion and capillary action to enhance its swelling rate.[28]

Table I. Swelling Kinetic Parameters for the Superabsorbent Nanocomposites with Different Contents of I/S

Sample	Q_{eq} (g g^{-1})	Q_{∞} (g g^{-1})	K_{is} (g g^{-1} s^{-1})	R
I/S: 0%	680	689	8.029	0.9999
I/S: 2.5%	810	826	11.385	0.9999
I/S: 5%	703	714	8.003	0.9998
I/S: 10%	645	657	9.617	0.9998
I/S:15%	600	613	7.342	0.9998

K_{is}: The initial swelling rate constant (g g^{-1} s^{-1}); R: Linear correlation coefficient.

Swelling Behaviors in Different Salt Solutions

The effect of salt solution on the swelling behaviors of the superabsorbents was evaluated in NaCl, $CaCl_2$, and $FeCl_3$ solutions (Figure 7). As can be seen, the order of swelling capacity in all salt solutions is: NaAlg-*g*-p(AA-*co*-St)/I/S (2.5 wt %) > NaAlg-*g*-p(AA-*co*-St) > NaAlg-*g*-p(AA-*co*-St)/I/S (10 wt %). This was in accordance with the order in distilled water. Moreover, the increasing concentration of all salt solutions decreased the water absorption. This was ascribed to the fact

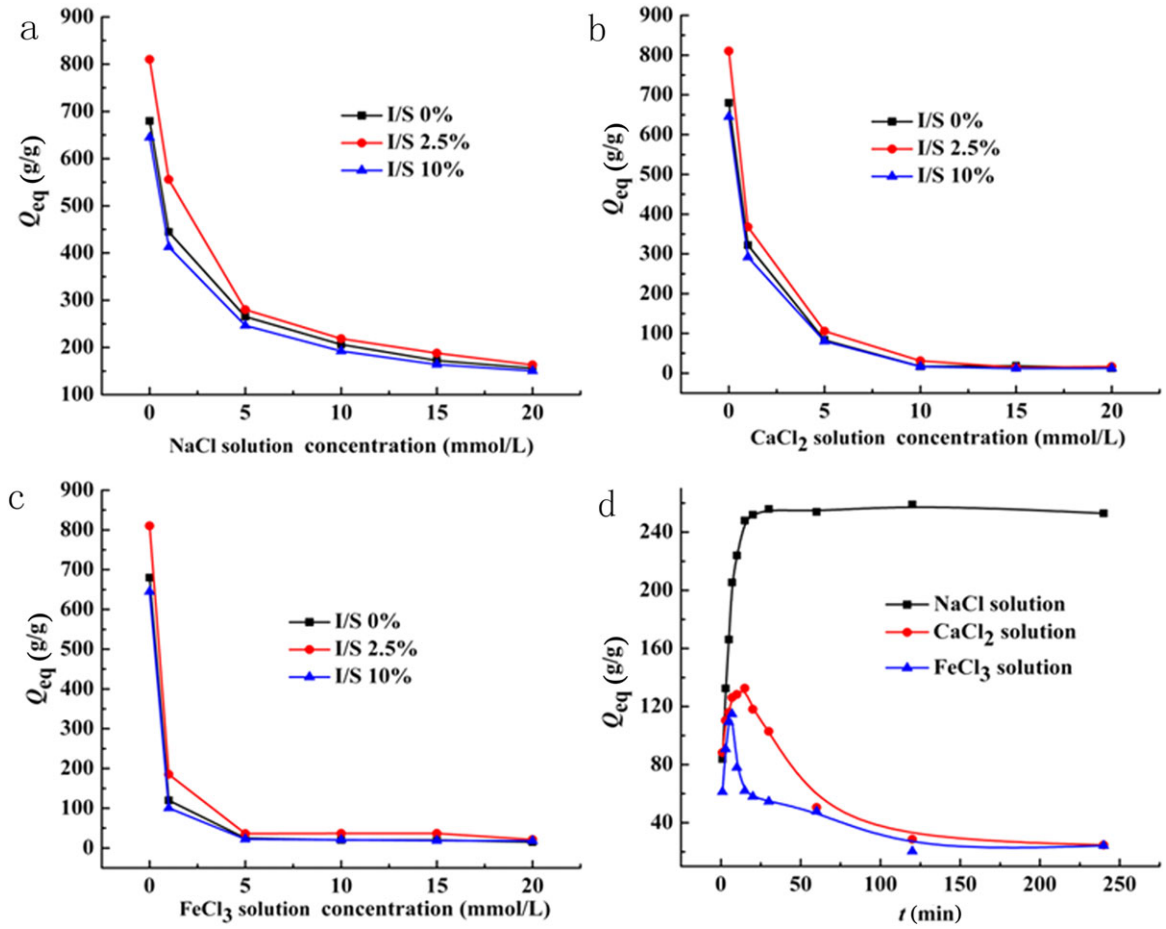

Figure 7. Effect of salt concentration on swelling ratio of the nanocomposites (a–c) and swelling kinetics of the optimized nanocomposite in 5 mmol/L salt solutions (d). [Color figure can be viewed in the online issue, which is available at wileyonlinelibrary.com.]

that osmotic pressure difference between the polymeric network and external solution was rapidly decreased, and the hydrogel was fleetly shrinked.[29] In addition, the multivalent cations in the salt solutions ($CaCl_2$ and $FeCl_3$) generated interchain complexing action with the carboxylate groups, which enhanced the network crosslink density. Consequently, the swelling ratio of the superabsorbents in various salt solutions followed the order of NaCl > $CaCl_2$ > $FeCl_3$.

Figure 7(d) shows the influence of various salts on the kinetic swelling characteristics of the optimized nanocomposite containing 2.5 wt % I/S. Unlike in NaCl solution, the nanocomposite exhibited swelling–deswelling-equilibrium phenomenon in $CaCl_2$ and $FeCl_3$ solutions. This is actually known as the "overshoot effect"; the swelling ratio of the nanocomposite reached the maximum value within 15 min in $CaCl_2$ solution and 7 min in $FeCl_3$ solution and then decreased to the equilibrium value. This can be explained by that the complexation interactions between the multivalent cations and the carboxylate groups tended to hinder the expanding of polymer network and to expel the water holded in network spaces.

Swelling Behaviors in Various Surfactant Solutions

Figure 8 represents the swelling properties of NaAlg-*g*-p(AA-*co*-St)/I/S (2.5 wt %) superabsorbent nanocomposite in the aqueous solutions of cationic and anionic surfactants with various concentrations. It can be observed that the swelling ratio decreased with increasing surfactant concentration, but the decreasing degree was more obvious in the DTAB and CTAB solution than that in the SDS solution. In SDS solution, the anionic SDS molecules are difficult to enter the polymer network, because it may repulse with the negatively charged carboxylate groups of the polymer chains, and so SDS has only slight influence on the swelling properties. Different from SDS, the cationic DTAB and CTAB molecules have greater influence on the swelling properties due to the following reasons: (1) the ionic surfactant could self-assemble in crosslinked polyelectrolyte gel with counter charges and form a liquid crystal of surfactant aggregates, and then caused the shrinkage of the nanocomposite[30–32]; (2) the positively charged DTAB and CTAB molecules easily associated with negatively charged carboxylate groups, this is unfavorable for the expansion of the polymeric network; (3) the hydrophobic interaction of long alkyl chains in hydrogel network weakened the hydrophilicity of the nanocomposite.

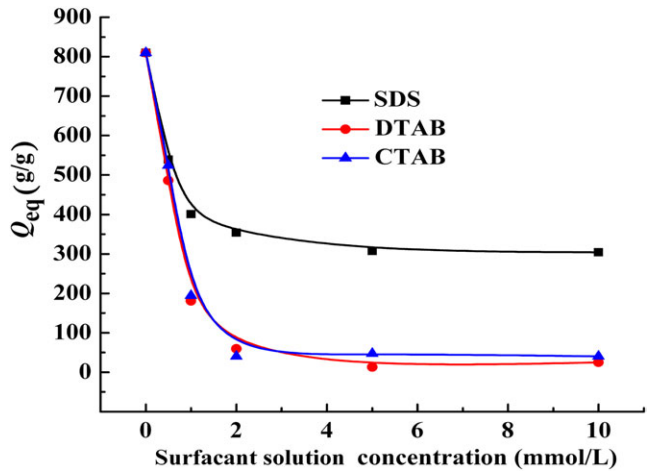

Figure 8. Effect of surfactant solutions on swelling ratio the optimized nanocomposite. [Color figure can be viewed in the online issue, which is available at wileyonlinelibrary.com.]

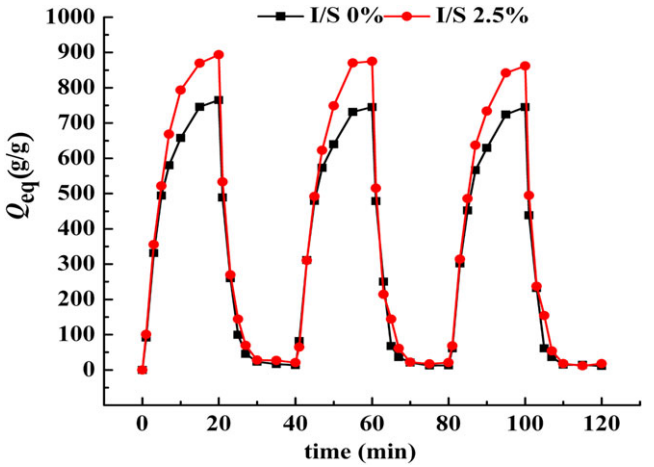

Figure 9. On–off switching behavior of the nanocomposites as reversible pulsatile swelling (pH 7.0) and deswelling (pH 2.0). [Color figure can be viewed in the online issue, which is available at wileyonlinelibrary.com.]

Evaluation of pH-Responsivity

In this section, the pH-responsivity of NaAlg-*g*-p(AA-*co*-St) and NaAlg-*g*-p(AA-*co*-St)/I/S (2.5 wt %) were characterized by the swelling–deswelling cycles between the buffer solutions of pH 7.0 and 2.0. As shown in Figure 9, the hydrogels exhibited intriguing on–off switching behavior. In pH 7.0 medium, the sample achieved higher swelling because of the anion–anion repulsive electrostatic forces among carboxylate groups, while the swollen gel rapidly deswelled after being soaked in pH 2.0 buffer solutions due to the protonation of $-COO^-$ groups in acidic medium. Moreover, the NaAlg-*g*-p(AA-*co*-St)/I/S (2.5 wt %) had bigger amplitude of swelling than the I/S-free hydrogel. This indicated that pH-responsivity was improved by the introduction of proper amount of I/S clay, which endow the nanocomposite more suitable as a potential candidate for drug delivery.[33]

CONCLUSION

To reduce the excessive consumption of petroleum products and the environmental impact resulting from industrial polymers, a series of novel NaAlg-*g*-P(AA-co-St)/I/S superabsorbent nanocomposites with enhanced water absorption were synthesized in aqueous solution by using APS as a radical initiator and MBA as a crosslinker. FTIR spectra proved that AA and St comonomers have been grafted onto NaAlg backbones, and I/S participated in copolymerization. XRD and SEM observations revealed that I/S was exfoliated thoroughly and uniformly dispersed in the polymer matrix. The water absorption and swelling rate were significantly improved by introduction of 2.5 wt % I/S. The nanocomposites showed distinct water absorption in salt solution with various valences and exhibited intriguing swelling–deswelling behaviors in $CaCl_2$ and $FeCl_3$ solutions. The

result about the effect of surfactant solutions on swelling of the nanocomposite indicated that the anionic surfactant had less influence on the water absorption than cationic surfactant. In addition, compared with I/S-free superabsorbent, the nanocomposite had better pH-responsivity and can be more suitable for drug delivery carrier.

ACKNOWLEDGMENTS

The authors thank the Science and Technology Support Project of Jiangsu Provincial Sci. & Tech. Department (No. BY2010012) and Jiangsu Provincial Joint Innovation and Research Funding of Enterprises, Colleges and Institutes—Prospective Cooperative Research Project (No. BY2011194) for the financial support of this research.

REFERENCES

1. Wang, Y. F.; Liu, M. Z.; Ni, B. L.; Xie, H. L. *Ind. Eng. Chem. Res.* **2012**, *51*, 1413.
2. Kosemund, K.; Schlatter, H.; Ochsenhirt, J. L.; Krause, E. L.; Marsman, D. S.; Erasala, G. N. *Regul. Toxicol. Pharm.* **2008**, *53*, 81.
3. Das, A.; Kothari, V. K.; Makhija, S.; Avyaya, K. *J. Appl. Polym. Sci.* **2008**, *107*, 1466.
4. Karadag, E.; Uzum, O. B. *Polym. Bull.* **2012**, *68*, 1357.
5. Tang, Q. W.; Lin, J. M.; Wu, J. H.; Huang, M. L. *Eur. Polym. J.* **2007**, *43*, 2214.
6. Wang, Q.; Zhang, J. P.; Wang, A. Q. *Carbohydr. Polym.* **2009**, *78*, 731.
7. Zou, W.; Yu, L.; Liu, X. X.; Chen, L.; Zhang, X. Q.; Qiao, D. L.; Zhang, R. Z. *Carbohydr. Polym.* **2012**, *87*, 1583.
8. Saber-Samandari, S.; Gazi, M.; Yilmaz, E. *Polym. Bull.* **2012**, *68*, 1623.
9. Wang, W. B.; Wang, Q.; Wang, A. Q. *Macromol. Res.* **2011**, *19*, 57.
10. Abd Alla, S. G.; Sen, M.; El-Naggar, A. W. M. *Carbohydr. Polym.* **2012**, *89*, 478.
11. Li, J.; Ji J.; Xia, J.; Li, B. *Carbohydr. Polym.* **2012**, *87*, 757.
12. Wang, W. B.; Wang, A. Q. *Carbohydr. Polym.* **2009**, *77*, 891.
13. Anirudhan, T. S.; Tharun, A. R.; Rejeena, S. R. *Ind. Eng. Chem. Res.* **2011**, *50*, 1866.
14. Wang, W. B.; Wang, A. Q. *Carbohydr. Polym.* **2010**, *82*, 83.
15. Shi, X. N.; Wang, W. B.; Wang, A. Q. *J. Compos. Mater.* **2011**, *45*, 2189.
16. Pourjavadi, A.; Hosseinzadeh, H.; Sadeghi, M. *J. Compos. Mater.* **2007**, *41*, 2057.
17. Ray, S. S.; Bousmina, M. *Prog. Mater. Sci.* **2005**, *50*, 962.
18. Li, Z. Q.; Shen, J. F.; Ma, H. W.; Li, X.; Shi, M.; Li, N.; Ye, M. X. *Polym. Bull.* **2012**, *68*, 1153.
19. Xia, C. P.; Xiao, C. M. *J. Appl. Polym. Sci.* **2012**, *123*, 2244.
20. Reynold, R. C. *Clay Clay Miner.* **1992**, *40*, 387.
21. Miroslav, H.; Norbert, C.; Vladimír, Š. *Chem. Geol.* **2008**, *249*, 167.
22. Shi, X. N.; Wang, W. B.; Kang, Y. R.; Wang, A. Q. *J. Appl. Polym. Sci.* **2012**, *125*, 1822.
23. Burnside, S. D.; Giannelis, E. P. *Chem. Mater.* **1995**, *7*, 1597.
24. Luo, W.; Zhang, W.; Chen, P.; Fang, Y. *J. Appl. Polym. Sci.* **2005**, *96*, 1341.
25. Wang, W. B.; Wang, A. Q. *J. Compos. Mater.* **2009**, *43*, 2805.
26. Schott, H. *J. Macromol. Sci. B* **1992**, *31*, 1.
27. Bajpaia, S. K.; Johnson, S. *React. Funct. Polym.* **2005**, *62*, 271.
28. Omidian, H.; Hashemi, S. A.; Sammes, P. G. *Polymer* **1999**, *40*, 1753.
29. Buchanan, K. J.; Hird, B.; Letcher, T. M. *Polym. Bull.* **1986**, *15*, 325.
30. Hansson, P. *Langmuir* **1998**, *14*, 2269.
31. Hansson, P.; Lindman, B. *J. Phys. Chem. B* **2002**, *106*, 9777.
32. Svensson, A.; Piculell, L.; Karlsson, L.; Cabane, B.; Jonsson, B. *J. Phys. Chem. B* **2002**, *106*, 1013.
33. Sadeghi, M.; Yarahmadi, M. *Afr. J. Biotechnol.* **2011**, *10*, 12265.